

See discussions, stats, and author profiles for this publication at: <https://www.researchgate.net/publication/255758530>

Robust synthesis of gold rhombic dodecahedra with well-controlled sizes and their optical properties

ARTICLE in CRYSTENGCOMM · DECEMBER 2012

Impact Factor: 4.03 · DOI: 10.1039/C2CE25598G

CITATIONS

6

READS

77

6 AUTHORS, INCLUDING:



[Do Youb Kim](#)

Korea Research Institute of Chemical Tech...

42 PUBLICATIONS 684 CITATIONS

[SEE PROFILE](#)



[Sang Hyuk Im](#)

Kyung Hee University

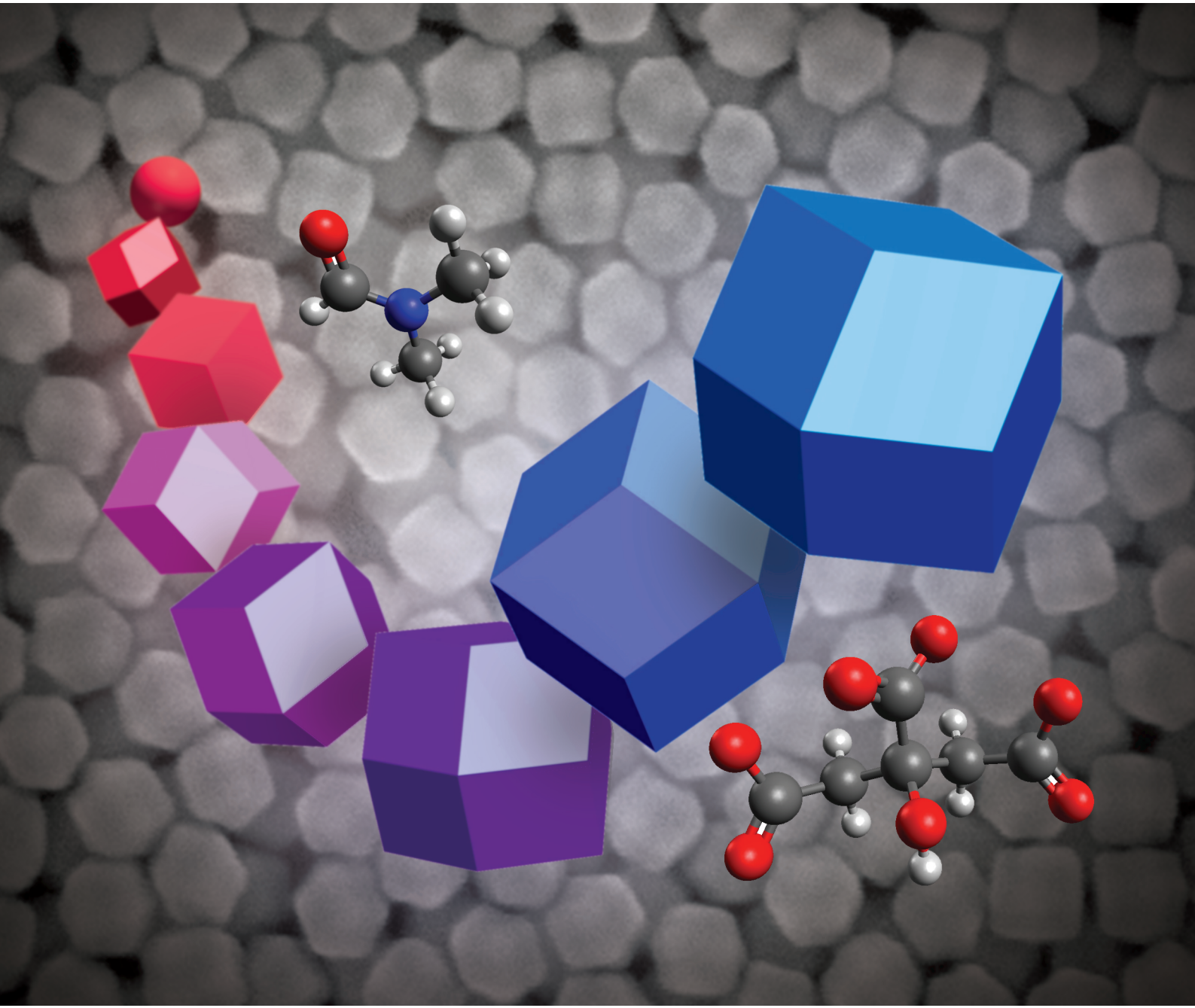
199 PUBLICATIONS 9,282 CITATIONS

[SEE PROFILE](#)

CrystEngComm

www.rsc.org/crystengcomm

Volume 15 | Number 2 | 14 January 2013 | Pages 215–422



PAPER

Sang Hyuk Im, O Ok Park *et al.*

Robust synthesis of gold rhombic dodecahedra with well-controlled sizes and their optical properties

RSC Publishing

PAPER

Robust synthesis of gold rhombic dodecahedra with well-controlled sizes and their optical properties^t

Cite this: *CrystEngComm*, 2013, 15, 252

Kyeong Woo Choi,^{‡,a} Do Youb Kim,^{‡,a} Xiao-Lan Zhong,^b Zhi-Yuan Li,^b Sang Hyuk Im^{*c} and O Ok Park^{*ad}

Received 19th April 2012,
Accepted 28th May 2012

DOI: 10.1039/c2ce25598g

www.rsc.org/crystengcomm

Through the seed-mediated growth method in *N,N*-dimethylformamide (DMF)–water medium using trisodium citrate and poly(vinyl pyrrolidone) (PVP) as stabilizer, Au rhombic dodecahedra with a narrow size distribution (< 5% in standard deviation) and high shape yield (> 90%) could be reproducibly synthesized thanks to the robust formation of rhombic dodecahedra by DMF–water medium and surface stabilization by trisodium citrate. Moreover, the edge lengths of these Au rhombic dodecahedra could be readily controlled from 19 to 67 nm by varying the amount of seeds, concentration of HAuCl₄, or both, and thus the localized surface plasmon resonance peak positions of the Au rhombic dodecahedra could be continuously tuned from 532 to 655 nm.

Introduction

Gold (Au) nanocrystals have attracted tremendous attention in recent decades due to their fascinating properties, such as localized surface plasmon resonance (LSPR), bio-compatibility, easy surface modification, and catalytic activity.^{1–4} These remarkable properties have enabled many important applications in sensors, photonics, electronics, catalysis, and biomedicine.^{5–11} Because the shape and size of nanocrystals strongly affects their physical, optical, electronic, and catalytic properties, as well as their magnetic properties, morphological control of Au nanocrystals is very important.^{12–16} In these regards, there has been a great deal of effort to generate Au nanocrystals with controlled shapes and sizes.^{14–18}

A rich variety of solution-phase methods have been demonstrated for generating Au nanocrystals with different morphologies, including spheres, cubes, octahedra, deca-

dra, icosahedra, rods, and plates.^{14–18} However, most morphologies have been restricted to those enclosed by low-index facets, {111} and/or {100} facets, which possess relatively lower surface energy in a face-centered cubic (*fcc*) metal. It is generally understood that newly formed metal atoms preferentially nucleate and grow from the already formed nanocrystals' surfaces with higher surface energies to minimize the total surface energy of nanocrystals.^{19,20} These high energy surfaces thus easily disappear during the growth of nanocrystals, consequentially generating nanocrystals enclosed by lower surface energies. The synthesis of Au nanocrystals enclosed by high energy surfaces is therefore considered to be difficult as compared to the synthesis of nanocrystals enclosed by low energy surfaces. Accordingly, there have been few reports of Au nanocrystals exclusively enclosed by {110} facets, termed rhombic dodecahedra, because {110} facets have the highest surface energy among the low-index facets in *fcc* metals and usually disappear during the crystal growth. There have been several attempts to obtain rhombic dodecahedral Au nanocrystals with well-defined morphology and rational manipulation of growth.^{21–26} For example, Jeong *et al.*²¹ demonstrated the synthesis of Au rhombic dodecahedra *via* a one-step process by reduction of HAuCl₄ in DMF and water at 90–95 °C, and we²² also reported that the rhombic dodecahedra could be transformed to octahedra *via* rhombic-cuboctahedra in DMF–water medium. However, the resultant Au rhombic dodecahedra exhibited rather poor uniformity of morphology and their size could not be controlled, especially for relatively smaller ones. Recently, Niu *et al.*²³ and Huang *et al.*^{11,24,25} successfully synthesized Au rhombic dodecahedra *via* a seed-mediated growth method of which the size and shape is sensitive to the ratio of substrates: shapes can be transformed from rhombic dodecahedra to octahedra (or

^aDepartment of Chemical and Biomolecular Engineering (BK21 graduate program), Korea Advanced Institute of Science and Technology (KAIST), 291 Daehakro, Yuseong-gu, Daejeon, 305-701, Korea. E-mail: ookpark@kaist.ac.kr; Fax: +82-42-350-3910; Tel: +82-42-350-3923

^bInstitute of Physics, Chinese Academy of Sciences, Beijing, 100190, China. E-mail: lizy@aphy.iphy.ac.cn; Tel: +86-10-8264-8106

^cKRICT-EPFL Global Research Laboratory, Advanced Materials Division, Korea Research Institute of Chemical Technology (KRICT), 19 Singsungno, Yuseong-gu, Daejeon, 305-600, Korea. E-mail: imromy@kRICT.re.kr

^dDepartment of Energy Systems Engineering, Daegu Gyeongbuk Institute of Science and Technology (DGIST), 50-1, Sangri, Hyeonpung-myeon, Dalseong-gun, Daegu, 711-873, Korea

^t Electronic supplementary information (ESI) available: TEM and HRTEM images of spherical Au seeds, UV-vis extinction spectrum of spherical Au seeds, and the plot of the calculated and experimentally measured LSPR peak position as a function of the edge length of Au rhombic dodecahedra. See DOI: 10.1039/c2ce25598g

[‡] These authors equally contributed to this work.

cubes) *via* transitional structures. Although above methods have strong advantages to synthesize Au nanocrystals with various shapes including rhombic dodecahedron, if we focus on the synthesis of Au rhombic dodecahedra with narrow size distribution and high shape yield, the DMF–water solution medium as a reducing agent and a solvent will be robust because its oxidative product can form the Au rhombic dodecahedra in an early stage of the reaction even under various reaction conditions.^{22,27} To exploit the potential robustness of DMF–water medium and to obtain Au rhombic dodecahedra with uniform and controllable morphology, here, the seed-mediated growth was adopted in DMF–water medium using PVP and trisodium citrate as a stabilizer. By varying the amount of seeds, the concentration of HAuCl₄, or both, we could systematically control the size of Au rhombic dodecahedra over a relatively broad range of 19–67 nm in edge length and reproducibly produce the Au rhombic dodecahedra with a narrow size distributions (< 5% in a standard deviation), and in high percentages (> 90% for the as-prepared samples).

Experimental section

Chemicals

Gold(III) chloride trihydrate (HAuCl₄·3H₂O, ≥ 99.9%), *N,N*-dimethylformamide (DMF, 99%), sodium borohydride (NaBH₄, 99%), L-ascorbic acid (AA, > 99%), poly(vinyl pyrrolidone) (PVP, $M_w \approx 55\,000$), cetyltrimethylammonium bromide (CTAB, ≥ 99%), cetyltrimethylammonium chloride (CTAC, ≥ 98%), and sodium citrate tribasic dehydrate (≥ 99%) were all obtained from Sigma-Aldrich and used as received. In all experiments, we used deionized water with a resistivity of 18.2 MΩ, prepared using an ultrapure water system (Human).

Synthesis of spherical Au seeds

The single-crystal spherical Au seeds were prepared using a two-step procedure.^{28,29} We first prepared 3-nm Au nanocrystallites by adding 0.6 mL of 10 mM ice-cold NaBH₄ aqueous solution to 10 mL of an aqueous solution containing 0.25 mM of HAuCl₄ and 0.1 M CTAB, generating a brownish solution. The seed solution was kept undisturbed for 3 h at 27 °C to ensure complete decomposition of NaBH₄ remaining in the solution. Second, 6 mL of 0.5 mM HAuCl₄, 6 mL of 0.2 M CTAC and 4.5 mL of 0.1 M AA aqueous solutions were mixed in a glass vial, followed by the addition of 0.3 mL of the as-prepared suspension of 3 nm Au nanocrystallites. The final mixture turned from colorless to red within 1 min, indicating the formation of larger Au nanoparticles. After 1 h, the products were collected by centrifugation (14 500 rpm, 30 min) and then washed with water once. The as-obtained spherical Au seeds were *ca.* 10 nm in diameter and they were re-dispersed in water. As determined by using an inductively-coupled plasma atomic emission spectrometer (ICP-AES, Optima 7300 DV, Perkin-Elmer) and TEM imaging, the concentration of Au in the seed solution was 282 mg L⁻¹ (the corresponding Au nanocrystal concentration was 2.6 × 10¹⁶ particles L⁻¹).

Synthesis of Au rhombic dodecahedra

In a standard synthesis, 0.5 M of trisodium citrate aqueous solution (0.3 mL) and water (0.14 mL) were mixed with DMF (11.5 mL) containing HAuCl₄ (0.819 mM) and PVP (8.63 mM), followed by the addition of 60 µL of Au seed solution (2.6 × 10¹⁶ particles L⁻¹) in a 50 mL glass vial. The molar concentration of PVP was calculated in terms of the repeating unit. The vial was then capped and heated in an oil bath at 70 °C for 3 h under magnetic stirring. The product was subsequently collected by centrifugation at 12 000 rpm for 5 min, and then washed with water and ethanol several times. The product was finally re-dispersed in ethanol for further characterization. To obtain Au rhombic dodecahedra with different sizes, the amount of Au seeds or the concentration of HAuCl₄ was varied, while the other reaction conditions were kept the same.

Characterization

Scanning electron microscopy (SEM) images were recorded with a field-emission scanning microscope (Sirion, FEI) operated at an accelerating voltage of 20 kV. Transmission electron microscopy (TEM) images were recorded with a transmission electron microscope (JEM-3011, JEOL) operated at an accelerating voltage of 300 kV. High-resolution TEM (HRTEM) images were recorded with a field-emission transmission electron microscope (Tecnai G2 F30 S-Twin, FEI) operated at an accelerating voltage of 300 kV. The samples were prepared by placing a few drops of the colloidal suspension in ethanol either on silicon substrates for SEM or on copper grids coated with carbon for TEM and HRTEM. The UV-vis spectra were recorded with a UV-vis spectrometer (Cary 100, Varian) with the particles suspended in ethanol. The concentration of Au was determined by ICP-AES and converted to the number of Au nanocrystals. The sample for ICP-AES was prepared by dissolving the Au particles in a mixture of hydrochloric acid (HCl, 37% in volume, 0.3 mL) and nitric acid (HNO₃, 70% in volume, 0.1 mL), followed by dilution with water until the HCl content reached 2% (volume) in the final solution.

Result and discussion

Synthesis and characterization of Au rhombic dodecahedra

The synthesis of the Au rhombic dodecahedra involves two steps. In the first step, Au nanospheres with a diameter of *ca.* 10 nm, which were used as seeds for preparing Au rhombic dodecahedra, were prepared by following the protocol reported in the literature.^{28,29} Briefly, Au nanocrystallites of approximately 3 nm diameter were prepared in water by reduction of HAuCl₄ with NaBH₄ in the presence of CTAB at room temperature. These Au nanocrystallites were then allowed to grow into Au nanospheres with a larger and more uniform size in the presence of additional HAuCl₄, AA and CTAC at room temperature. Fig. S1A† in the ESI shows a typical TEM image of as-prepared Au nanospheres, which were highly uniform in both size (10.2 nm ± 0.6 nm) and shape. Fig. S1B† in the ESI shows a HRTEM image and the corresponding fast

Fourier transform (FFT) pattern (inset of Fig. S1B† in the ESI) of an individual Au nanosphere, indicating its single-crystalline nature. Since an Au rhombic dodecahedron has a single-crystalline structure, it is critical to prepare Au seeds with a single-crystalline structure in high percentage in order to obtain Au rhombic dodecahedra in high percentage. The percentage of single crystals among as-prepared Au seeds exceeded 96%.

In the second step, Au rhombic dodecahedra were prepared using 10 nm Au nanospheres as seeds, which were prepared in the first step. For a standard synthesis, 60 μ L of as-prepared Au seed suspension (2.6×10^{16} particles L^{-1}) was added to a mixed solution of DMF (11.5 mL) and water (0.44 mL) that contained HAuCl₄ (0.79 mM), PVP (8.3 mM, in terms of repeating unit) and trisodium citrate (12.6 mM) at room temperature. This mixed solution was then capped and heated in an oil bath at 70 °C for 3 h under magnetic stirring. Fig. 1A and Fig. 1B show typical SEM and TEM images of as-prepared Au rhombic dodecahedra, which had an edge length of 35.3 ± 1.0 nm and could be obtained in high percentage (> 90%) without any additional purification. As shown in the SEM and TEM images, the morphology of the Au nanocrystals was not that of a perfect rhombic dodecahedron, but instead was characterized by slightly protruded vertices, indicating that the as-prepared Au rhombic dodecahedra were enclosed by mix of {110} and its vicinal facets on the surface. The HRTEM image taken from an individual Au rhombic dodecahedron (Fig. 1C) shows continuous fringes with spacing of 0.235, 0.204 and 0.144 nm, which could be indexed to the {111}, {200} and {220} reflections of fcc Au, respectively. The corresponding selective area electron diffraction (SAED) pattern (inset of Fig. 1C) confirms the single-crystal nature of the nanocrystal, indicating that this nanocrystal was situated on the TEM grid along the [011] zone axis.^{22,23} Fig. 1D shows schematic drawings of a rhombic dodecahedron in four different orientations that

correspond to those of the nanocrystals marked with the same numbers in Fig. 1A.

Taking advantages of seed-mediated growth method, we could easily control the size of Au rhombic dodecahedra in a relatively broad range from 19.0 nm to 67.2 nm in edge length by varying the amount of seed, concentration of HAuCl₄, or a combination of these. Fig. 2 shows TEM images of Au rhombic dodecahedra with different edge lengths obtained by adding different volumes of Au seed solution into each set of reaction solutions containing the same concentration of HAuCl₄. The edge length of the resultant Au rhombic dodecahedra increased from 19.0 to 24.3, 29.8, 35.3, 41.2, 46.1, 55.9 and 67.2 nm, when the volume of the Au seed solution (2.6×10^{16} particles L^{-1}) was reduced from 200 to 110, 80, 60, 40, 30, 20 and 15 μ L, respectively. As shown in the TEM images, Au rhombic dodecahedra in all samples were uniform in both shape and size, which can be considered an outcome of the uniform single-crystalline Au seeds. It was found that the relatively small rhombic dodecahedra were rounded at the corners (inset of Fig. 2A), while larger rhombic dodecahedra had protruded vertices (Fig. 2E and Fig. 2F) compared to the perfect rhombic dodecahedron.

The size of resultant Au rhombic dodecahedra could be also readily controlled by changing the concentration of HAuCl₄, while the amount of Au seeds was kept the same. Fig. 3A shows the TEM image of Au rhombic dodecahedra with an edge length of 27.3 nm, obtained by using the standard procedure, except that the concentration of HAuCl₄ was reduced from 0.785 mM to 0.55 mM. When the concentration of HAuCl₄ was increased to 1.57 mM, Au rhombic dodecahedra with an edge length of 51.7 nm were obtained (Fig. 3B). The Au rhombic dodecahedra obtained by varying the concentration of HAuCl₄ with the same number of Au seeds were also uniform in both shape and size. Table 1 summarizes the average edge length, standard deviation, and percentage of Au rhombic dodecahedra in the as-prepared product. We can conclude that Au rhombic dodecahedra with a broad range of sizes (19.0–67.2 nm in edge length) could be readily prepared with narrow size distributions (<5% in standard deviation) and in high percentages (>90% for the as-obtained samples).

We further investigated the influence of water, trisodium citrate, and the reaction temperature on the final morphology of the Au nanocrystals. In the reaction system, which uses DMF as a reducing agent, water is essential for the oxidation of DMF,—and thus the reduction of metal ions into atoms—and the amount of water is critical for the formation of Au nanocrystals.^{22,28} In order to elucidate the effect of water on the formation of Au nanocrystals, we conducted control experiments using different amounts of water in the reaction solution, while the other reaction conditions were kept the same as in the standard synthesis. When a relatively small amount of water (0.36 or 0.5 mL) was introduced into the reaction solution, Au rhombic dodecahedra with an edge length of ca. 35 nm were obtained, as shown in Fig. 1 and Fig. 4A. As the amount of water was increased to 1.0 mL, as-obtained Au nanocrystals exhibited a mixture of smaller Au rhombic dodecahedra (ca. 19 nm in edge length) and irregular Au nanocrystals with twinned structures (Fig. 4B). When the amount of water was 1.5 mL, most of the resultant Au

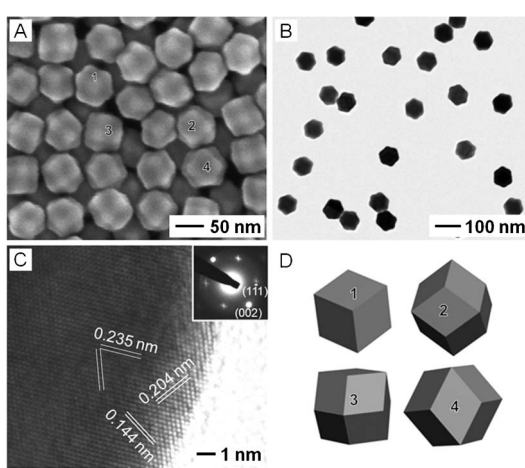


Fig. 1 (A) SEM and (B) TEM images of Au rhombic dodecahedra prepared using the standard procedure. (C) HRTEM image taken from the edge region of a rhombic dodecahedron and the corresponding SAED pattern (inset). (D) Schematic drawings of a rhombic dodecahedron in four different orientations that correspond to those of nanocrystals marked with the same numbers in (A).

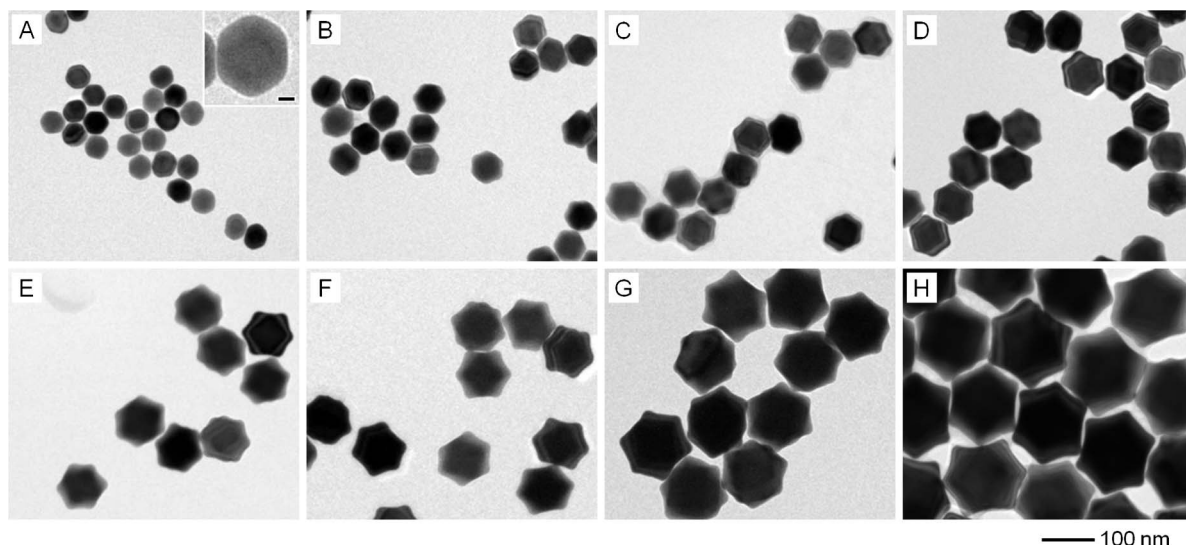
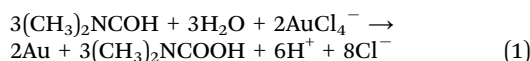


Fig. 2 TEM images of Au rhombic dodecahedra with different edge lengths prepared using the standard procedure except with different volumes (in parenthesis) of the Au seed solution: (A) 19.0 nm (200 μ L), (B) 24.3 nm (110 μ L), (C) 29.8 nm (80 μ L), (D) 35.3 nm (60 μ L), (E) 41.2 nm (40 μ L), (F) 46.1 nm (30 μ L), (G) 55.9 nm (20 μ L) and (H) 67.2 nm (15 μ L), respectively. The scale bar in the inset represents 10 nm.

nanocrystals exhibited irregular shape and size with twinned structures (Fig. 4C). In the present experimental system, DMF reduced HAuCl_4 in the presence of water to generate Au nanocrystals, and the reaction can be described as follows:³⁰



In this reaction, water can accelerate the reaction rate and lead Au ions to be reduced more quickly into Au atoms. It is believed that an increase in water content accelerated the reaction rate, causing homogeneous nucleation rather than heterogeneous nucleation of Au from the Au seeds, and consequentially generated multiply-twinned Au nanocrystals. It has also been reported that, for stable conformal overgrowth on seeds, the growth rate should be adequately low due to the kinetics of growth.³¹

We also found that the presence of trisodium citrate played a critical role in the formation of Au rhombic dodecahedra in

the present reaction system. Fig. 5 shows TEM images of Au nanocrystals obtained using the standard procedure except for the use of different concentrations of trisodium citrate. When trisodium citrate was excluded from the reaction mixture, relatively large and irregular Au particles with a size over 500 nm were obtained (Fig. 5A). It should be pointed out that the reaction mixture contained 8.25 mM of PVP, implying that PVP alone in a relatively small amount could not stabilize the seeds efficiently. When comparing the reaction conditions described in a previous report on the synthesis of Au octahedra under similar reaction conditions,²⁸ where 100 mM of PVP was required for efficient stabilization of Au seeds (with approximately twice the number that we used), the concentration level of 8.25 mM was relatively low. However, when a small amount of trisodium citrate (0.83 mM, 1/15 of the standard synthesis)

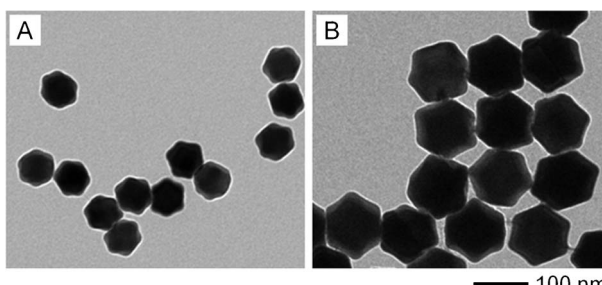


Fig. 3 TEM images of Au rhombic dodecahedra with different edge lengths prepared using the standard procedure except for the use of two different concentrations of HAuCl_4 (in parenthesis): (A) 27.3 nm (0.55 mM) and (B) 51.7 nm (1.57 mM), respectively.

Table 1 Average edge length (L_{av}), standard deviation (σ), and percentage of as-prepared Au rhombic dodecahedra using different volumes of Au seed solution, or different concentrations of HAuCl_4 solution.

Seed solution ^a [μ L]	L_{av} [nm]	σ [%]	Percentage of RD ^b [%]
200	19.0	4.7	90
110	24.3	4.9	91
80	29.8	3.3	92
60	35.3	2.8	92
40	41.2	2.9	92
30	46.1	3.0	91
20	55.9	3.2	90
15	67.2	4.9	88

HAuCl_4 ^c [mM]	L_{av} [nm]	σ [%]	Percentage of RD [%]
0.55	27.3	4.8	91
1.57	51.7	3.3	90

^a The concentration of HAuCl_4 was 0.785 mM. ^b RD denotes a rhombic dodecahedron. ^c The volume of Au seed solution was 60 μ L.

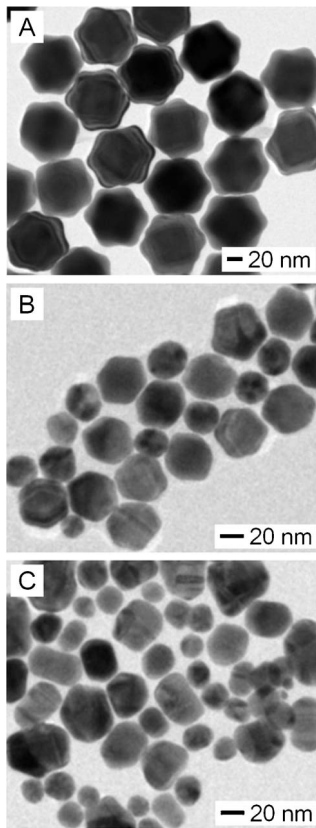


Fig. 4 TEM images of Au nanocrystals obtained with the standard procedure except for containing different amounts of water: (A) 0.36 mL, (B) 1.0 mL and (C) 1.5 mL.

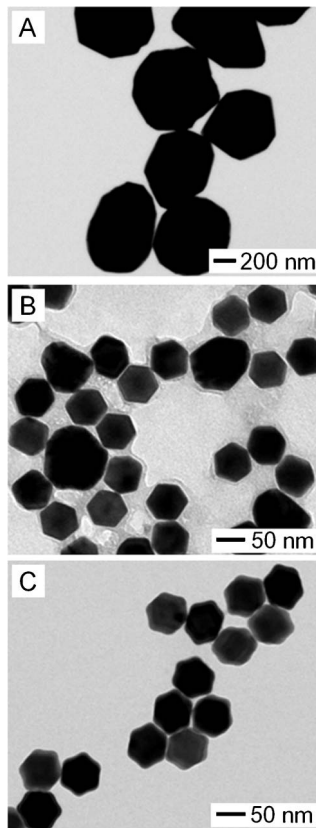


Fig. 5 TEM images of Au nanocrystals prepared using the standard procedure except (A) no use of trisodium citrate and (B–C) use of trisodium citrate with different concentrations: (B) 0.83 mM and (C) 1.25 mM.

was introduced into the reaction solution, Au rhombic dodecahedra with an edge length of *ca.* 30 nm were obtained together with irregular Au nanocrystals with a diameter of *ca.* 100 nm (Fig. 5B). The percentage of Au rhombic dodecahedra in this sample was <55%. The larger Au nanocrystals consumed a greater quantity of HAuCl₄, which can explain the slightly smaller size of the Au rhombic dodecahedra compared with those obtained using the standard procedure (Fig. 1B). When the concentration of trisodium citrate was over 1.25 mM (1/10 of the standard synthesis), Au rhombic dodecahedra with an edge length of *ca.* 35 nm were obtained in high percentage (>90%) (Fig. 5C). In the present reaction system, it is believed that trisodium citrate played roles in both stabilizing Au seeds to prevent Au seeds from aggregation and stabilizing {110} facets of Au nanocrystals by adsorbing on the surfaces of the Au nanocrystals. When the DMF adsorbed and stabilized {110} facets of Au in the early stage of the reaction and Au nanocrystals with rhombic dodecahedral shape were initially generated,^{22,27} trisodium citrate adsorbed on those {110} surfaces of Au nanocrystals and these relatively small Au rhombic dodecahedra grew larger, while maintaining their shape. Since the {110} surfaces have the highest surface energy among the three low-index faces,¹⁹ trisodium citrate could be adsorbed onto high energy facets such as the {110} surfaces of Au nanocrystals.

The influence of the reaction temperature on the morphology of the resultant Au nanocrystals was also verified. Fig. 6 shows TEM images of Au nanocrystals obtained using the standard procedure except under different reaction temperatures. When the reaction temperature was relatively low (*ca.* 25 °C), Au rhombic dodecahedra with sharp edges and corners were obtained after 10 h of reaction, where the reaction rate considerably decreased compared with the standard synthesis (Fig. 6A). On the contrary, Au rhombic dodecahedra with a highly rounded profile and/or nearly spherical Au nanocrystals were obtained at elevated reaction temperature (100 °C)

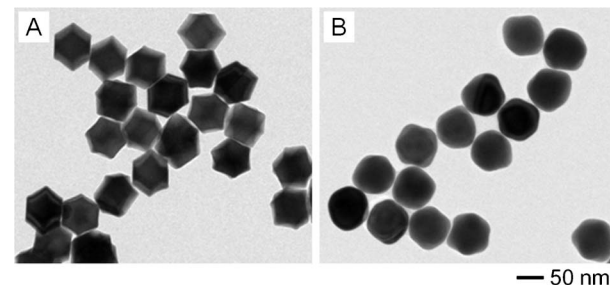


Fig. 6 TEM images of Au nanocrystals prepared using the standard procedure except under different reaction temperatures: (A) 25 °C and (B) 100 °C.

(Fig. 6B). It is known that the reduction process competes with the surface capping process by surfactants, and the relative rate of capping/decapping and relative growth rates along the different directions determine the shape of resultant nanocrystals.³² In addition, the reaction temperature can strongly influence the capping process and the reduction kinetics (thus the growth rate of nanocrystals) as well. It appears that when the reaction temperature was relatively low, the selective capping of trisodium citrate and DMF on the {110} facets of Au nanocrystals was dominant, and thus Au rhombic dodecahedra with sharp edges and corners formed. As the reaction temperature increased, however, the selective capping weakened and thermodynamic effects were dominant, and thus highly truncated or nearly spherical Au nanocrystals were generated. On the other hand, the Au nanocrystals enclosed by {110} facets are thermodynamically less favorable than their truncated forms, and they tended to evolve into Au nanocrystals with thermodynamically more favorable shapes at an elevated reaction temperature.

Optical properties of Au rhombic dodecahedra

The uniformity in shape and size as well as the ability to control the size of Au rhombic dodecahedra in a broad range allowed us to systematically investigate the dependence of their LSPR properties on size. The 10 nm Au nanospheres dispersed in water, used as seeds for preparing the Au rhombic dodecahedra in the present experiments, had an LSPR peak at 521 nm (Fig. S2† in the ESI). Fig. 7 shows typical UV-vis extinction spectra of Au rhombic dodecahedra with different edge lengths, which were dispersed in ethanol. As the edge length of Au rhombic dodecahedra gradually increased from 19.0 to 24.3, 29.8, 35.3, 41.2, 46.1, 55.9 and 67.2 nm, their LSPR peaks were red-shifted from 532 to 544, 554, 561, 574, 582, 615 and 655 nm, respectively. The LSPR peaks of Au rhombic dodecahedra with relatively small sizes (19.0 to 46.1 nm in edge length) were narrow and very sharp, which can be attributed to the uniformity of the Au rhombic dodecahedra in size and shape. As the edge length of Au rhombic dodecahedra increased to 55.9 nm, the dipole peak became broad and a shoulder appeared at around 550 nm. When the edge length of the Au rhombic dodecahedra was 67.2 nm, the LSPR peak broadened substantially and a shoulder was clearly observed. The broadening of the LSPR peak and the appearance of the shoulder could be attributed to the interactions between dipole resonances in larger Au nanocrystals,^{33,34} as well as the relatively wide size distributions of the Au rhombic dodecahedra with larger sizes. Fig. 7B shows a plot of the LSPR peak position as a function of the edge length of Au rhombic dodecahedra. As the edge length of the Au rhombic dodecahedra increased, the LSPR peak position was continuously red-shifted, but the trend was not well-fitted to a linear correlation between the LSPR peak position and the edge length of Au rhombic dodecahedra.

In order to clarify the LSPR properties of the Au rhombic dodecahedra according to their edge length, we calculated the extinction spectra of Au rhombic dodecahedra with similar edge lengths using the discrete dipole approximation (DDA) method. Fig. S3† in the ESI shows a plot of the theoretically calculated LSPR peak position as a function of the edge length

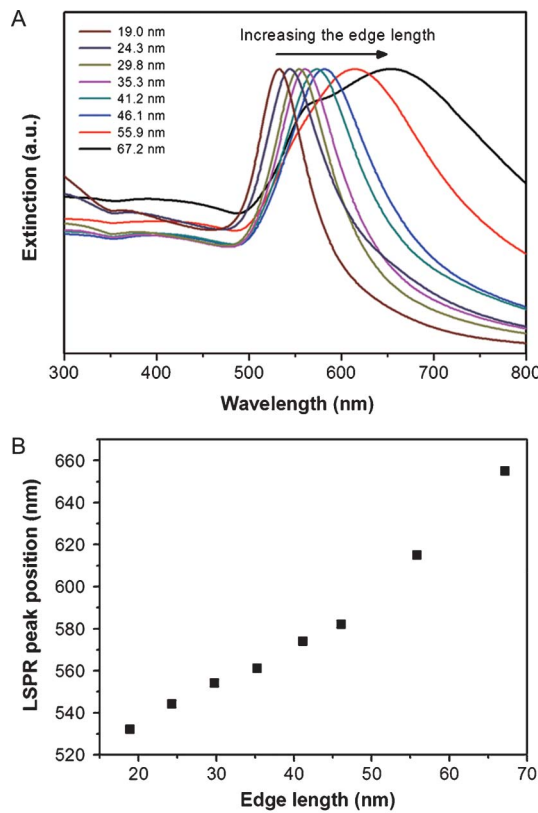


Fig. 7 (A) UV-vis extinction spectra of Au rhombic dodecahedra with different edge lengths. (B) Plot of the LSPR peak position as a function of the edge length of Au rhombic dodecahedra.

of perfect Au rhombic dodecahedra together with the experimentally measured LSPR peak position of the Au rhombic dodecahedra dispersed in ethanol. Comparing the experimentally measured LSPR peak positions with the calculated positions, a similar trend in the LSPR peak shift as a function of edge length was observed. The calculations reveal that the LSPR peak position does not show a linear relationship with edge length of an Au rhombic dodecahedron in the range of 19.5–67.5 nm. Moreover, when the edge lengths of Au rhombic dodecahedra are relatively large (56–67.5 nm), dipolar resonance peaks split into two distinct peaks with approximately equal intensities. It has been reported that the split and broadening of the LSPR peaks in larger nanocrystals are manifested by dipole interactions.^{33,34} We can also see that the LSPR peak positions for the as-obtained Au rhombic dodecahedra in all samples were relatively blue-shifted as compared with the theoretically calculated values for those with perfect rhombic dodecahedral shape. This can be attributed to some truncations at corners of obtained Au rhombic dodecahedra (Fig. 2), which is consistent with a previous report that the LSPR peak position is not only dependent on the size of the particles but also the degree of truncation at corners and it is gradually blue-shifted as the degree of truncation increases.²⁸

Conclusion

We have demonstrated the preparation of uniform Au rhombic dodecahedra in high percentage by seed-mediated growth. First, we obtained single-crystal Au nanospheres with a diameter of approximately 10 nm with a high percentage of over 96%. Uniform Au rhombic dodecahedra were then prepared by seeded growth with the Au nanospheres as seeds in DMF containing HAuCl₄, PVP, trisodium citrate and a small amount of water. The edge length of the resultant Au rhombic dodecahedra could be tightly controlled from 19 nm to 67 nm by varying the amount of Au seeds, the concentration of HAuCl₄, or both. The localized surface plasmon resonance peak positions of the Au rhombic dodecahedra could be continuously tuned from 532 to 655 nm depending on their sizes. The use of Au seeds with uniform shape and size allowed us to gain better understanding of the effects of various reaction parameters on the morphology of nanocrystals. We believe that Au rhombic dodecahedra with tunable sizes and optical properties could be useful in a variety of applications, such as surface-enhanced Raman scattering and biomedical applications.^{5–11}

Acknowledgements

This work was supported by WCU (World Class University) program through the National Research Foundation of Korea (NRF) funded by the Ministry of Education, Science and Technology (MEST) (R32-2008-000-10142-0). This research was also partially supported by the Public Welfare & Safety research program through the NRF funded by the MEST (2011-0028468).

References

- 1 K. L. Kelly, E. Coronado, L. L. Zhao and G. C. Schatz, *J. Phys. Chem. B*, 2003, **107**, 668.
- 2 C. J. Murphy, A. M. Gole, J. W. Stone, P. N. Sisco, A. M. Alkilany, E. C. Goldsmith and S. C. Baxter, *Acc. Chem. Res.*, 2008, **41**, 1721.
- 3 Y. C. Cao, R. Jin and C. A. Mirkin, *Science*, 2002, **297**, 1536.
- 4 N. Lopez and J. K. Nørskov, *J. Am. Chem. Soc.*, 2002, **124**, 11262.
- 5 N. L. Rosi and C. A. Mirkin, *Chem. Rev.*, 2005, **105**, 1547.
- 6 X. Huang, I. H. El-Sayed, W. Qian and M. A. El-Sayed, *J. Am. Chem. Soc.*, 2006, **128**, 2115.
- 7 T. F. Jaramillo, S.-H. Baeck, B. R. Cuenya and E. W. McFarland, *J. Am. Chem. Soc.*, 2003, **125**, 7148.
- 8 D. H. Wang, D. Y. Kim, K. W. Choi, J. H. Seo, S. H. Im, J. H. Park, O O. Park and A. J. Heeger, *Angew. Chem. Int. Ed.*, 2011, **50**, 5519.
- 9 H. Wang, C. S. Levin and N. J. Halas, *J. Am. Chem. Soc.*, 2005, **127**, 14992.
- 10 C. E. Talley, J. B. Jackson, C. Oubre, N. K. Grady, C. W. Hollars, S. M. Lane, T. R. Huser, P. Nordlander and N. J. Halas, *Nano Lett.*, 2005, **5**, 1569.
- 11 H.-L. Wu, H.-R. Tsai, Y.-T. Hung, K.-U. Lao, C.-W. Liao, P.-J. Chung, J.-S. Huang, I.-C. Chen and M. H. Huang, *Inorg. Chem.*, 2011, **50**, 8106.
- 12 J. P. Wilcoxon and B. L. Abrams, *Chem. Soc. Rev.*, 2006, **35**, 1162.
- 13 M.-C. Danniel and D. Astruc, *Chem. Rev.*, 2004, **104**, 293.
- 14 C. Burda, X. Chen, R. Narayanan and M. A. El-Sayed, *Chem. Rev.*, 2005, **105**, 1025.
- 15 Y. Xia, Y. Xiong, B. Lim and S. E. Skrabalak, *Angew. Chem. Int., Ed.*, 2009, **48**, 60.
- 16 A. R. Tao, S. Habas and P. Yang, *Small*, 2008, **4**, 310.
- 17 M. Grzelczak, J. Pérez-Juste, P. Mulvaney and L. M. Liz-Marzán, *Chem. Soc. Rev.*, 2008, **37**, 1783.
- 18 D. Seo, J. C. Park and H. Song, *J. Am. Chem. Soc.*, 2006, **128**, 14863.
- 19 Z. L. Wang, *J. Phys. Chem. B*, 2000, **104**, 1153.
- 20 Y. Xiong, B. J. Wiley and Y. Xia, *Angew. Chem., Int. Ed.*, 2007, **46**, 7157.
- 21 G. H. Jeong, M. Kim, Y. W. Lee, W. Choi, W. T. Oh, Q.-H. Park and S. W. Han, *J. Am. Chem. Soc.*, 2009, **131**, 1672.
- 22 D. Y. Kim, S. H. Im, O O. Park and Y. T. Lim, *CrystEngComm*, 2010, **12**, 116.
- 23 W. Niu, S. Zheng, D. Wang, X. Liu, H. Li, S. Han, J. Chen, Z. Tang and G. Xu, *J. Am. Chem. Soc.*, 2009, **131**, 697.
- 24 H.-L. Wu, C.-H. Kuo and M. H. Huang, *Langmuir*, 2010, **26**, 12307.
- 25 P.-J. Chung, L.-M. Lyu and M. H. Huang, *Chem.-Eur. J.*, 2011, **17**, 9746.
- 26 M. L. Personick, M. R. Langille, J. Zhang, N. Harris, G. C. Schatz and C. A. Mirkin, *J. Am. Chem. Soc.*, 2011, **133**, 6170.
- 27 D. Y. Kim, S. H. Im and O O. Park, *Cryst. Growth Des.*, 2010, **10**, 3321.
- 28 D. Y. Kim, W. Li, Y. Ma, T. Yu, Z.-Y. Li, O O. Park and Y. Xia, *Chem.-Eur. J.*, 2011, **17**, 4759.
- 29 Y. Ma, W. Li, E. C. Cho, Z. Li, T. Yu, J. Zeng, Z. Xie and Y. Xia, *ACS Nano*, 2010, **4**, 6725.
- 30 I. Pastoriza-Santos and L. M. Liz-Marzán, *Adv. Funct. Mater.*, 2009, **19**, 679.
- 31 F.-R. Fan, D.-Y. Liu, Y.-F. Wu, S. Duan, Z.-X. Xie, Z.-Y. Jiang and Z.-Q. Tian, *J. Am. Chem. Soc.*, 2008, **130**, 6949.
- 32 J. M. Petroski, Z. L. Wang, T. C. Green and M. A. El-Sayed, *J. Phys. Chem. B*, 1998, **102**, 3316.
- 33 B. J. Wiley, S. H. Im, Z.-Y. Li, J. McLellan, A. Siekkinen and Y. Xia, *J. Phys. Chem. B*, 2006, **110**, 15666.
- 34 C. Li, K. L. Shuford, M. Chen, E. J. Lee and S. O. Cho, *ACS Nano*, 2008, **2**, 1760.